Comparison of K_u- and C- Band Backscatter Time Series over Land

K. Scipal, W. Wagner, R. Kidd
Inst. of Photogrammetry and Remote Sensing, Vienna University of Technology, Austria, email: kscipal@ipf.tuwien.ac.at

Niels Ringelmann
Deutsches Zentrum für Luft- und Raumfahrt (DLR), Germany

***Abstract* - C- and K_u-band scatterometer backscatter time series are analysed and compared to meteorological data for two biomes, the African Steppe and the Scandinavian Boreal Forest. Observed characteristics of large scale scattering are inferred and discussed.**

I. Introduction

Over the past decades, numerous systems, space and airborne, measured backscatter in various polarizations and frequencies accompanied by an impressive progress of research. Beside the widely used SAR systems, scatterometers have gained considerable attention. Although initially designed for ocean applications, they are now recognized to be a promising tool to monitor processes related to the land surface hydrology, such as soil moisture, freeze/thaw cycles and precipitation events.

Due to the European heritage, science and technological development in Europe have largely been focused on C-band data. The availability of K_u-band radar data through NASA's QuikScat satellite gives us now the opportunity to study scattering effects in C- and K_U-band. Comparing data from both sensors and meteorological data gives a good impression relating to the geophysical processes influencing backscatter at the resolution of the scatterometer, this extends our knowledge about the scattering process. Further by simultaneous analysis of time series, insight into the potential and synergistic use of multipolarization and multifrequency data and their sensitivity to geophysical processes, with special emphasis on the land surface hydrology is attained.

II. Data

To study microwave backscatter over land, QuikScat SeaWinds and ERS scatterometer data were extracted for Finland, Europe (Boreal Forest) and Mali, Africa (Steppe). SeaWinds is a scanning dual spot beam scatterometer, launched in June 1999 aboard the QuikScat satellite [1]. Backscatter measurements are collected simultaneously at constant incidence angles of 46° and 54° with horizontal and vertical polarization respectively, using a scanning dish antenna operating at 13.4 GHz (K_U-band). The antenna has a footprint size of 7x25 km and scans over a swath of 1800 km, imaging thereby 90% of Earth's surface in one day. The satellite passes the test area of Mali approximately at 6:00 a.m. and 6:00 p.m. local time. The Finnish test site is passed at 5:00 a.m. and 8:00 p.m. local time. Due to the high latitudes of the latter test site, passing times can vary up to 2 hours. To reduce noise and speckle and such facilitate data interpretation, backscatter measurements within 12.5 km distance from a synoptic weather station were averaged for each orbit.

The ERS scatterometer operates at 5.3 GHz (C-band) vertical polarization. Backscatter measurements are collected over an incidence angle range from 18° to 57°. Global coverage is achieved within 3 to 4 days. The test site of Mali is passed at 11:00 a.m. and at 11:00 p.m. local time, the Finnish site at 11:30 a.m. and at 10:00 p.m. local time. To reduce noise and speckle, ERS scatterometer measurements collected within 36 km distance from a synoptic weather station were averaged using a hamming window with a width of 85 km [2]. To allow a comparison between both data sets ERS scatterometer data were extrapolated to incidence angles of 46° and 54° according to a method described by Wagner et al. [3].

In addition to the scatterometer data, synoptic weather observations for 12 stations in Mali and 21 stations in Finland are available. Meteorological data encompass daily minimum and maximum temperature, precipitation and snow depth records.

III. Empirical Observations

In the following section, K_u and C-band time series over two very specific biomes: the African Steppe and the Scandinavian Boreal Forest are discussed. Figures 1 and 2 show characteristic fractions of the two year time series for these regions.

A. African Steppe

Over the African Steppe backscatter is stable during the dry season, with the exception of extraordinary rainfalls. Single peaks, especially evident in the temporally dense K_u-

0-7803-7537-8/02/$17.00 (C) 2002 IEEE

band series, are well attributed to rainfall events. Backscatter does not increase immediately after the first rainfall events at the onset of the rainfall season. This may be explained by high evaporation rates at the beginning of the rainy season and sandy soils not able to retain moisture. After some weeks, when plenty of rain has fallen, σ^0 increases until the height of the rainfall season. The very similar temporal behavior of the C- and Ku-band time series is remarkable. Generally no distinct difference can be observed between C-band $\sigma^0_{VV}(54)$ and K_u-band $\sigma^0_{VV}(54)$; C-band $\sigma^0_{VV}(46)$ and K_u-band $\sigma^0_{HH}(46)$ show a constant difference of 1dB with lower C-band backscatter. Both the increase at the beginning of the rainfall season and the decrease after it, takes place more or less simultaneous in the two frequency bands, despite the fact that K_u-band is expected to be less sensitive to soil moisture and more sensitive to vegetation compared to C-band. One potential explanation may be the close link between soil moisture and vegetation in this region: Plants will start growing as soon as sufficient soil water becomes available; green plant cover will shade the soil surface keeping it moist.

B. Boreal Forest

Over the Boreal Forest, σ^0 is very stable for all polarizations and frequencies during the winter, characterized by temperatures well below 0°C. In K_u-band volume scattering of dry snow is expected to be the dominant scattering mechanism. Correspondingly, the signal is observed to increase from about –13 dB for the outer and –11 dB for the inner beam during fall to maximum values of –9 dB and –7dB respectively, even for shallow snow cover. The effect of snow is less pronounced in C-band, confirming the observation that dry snow is highly transparent in C-band [4]. However, single melting and refreezing events are also evident at C-band. Sudden changes in backscatter intensity are related to a change of the scattering mechanism from volume to surface scattering (wet snow, surface water).

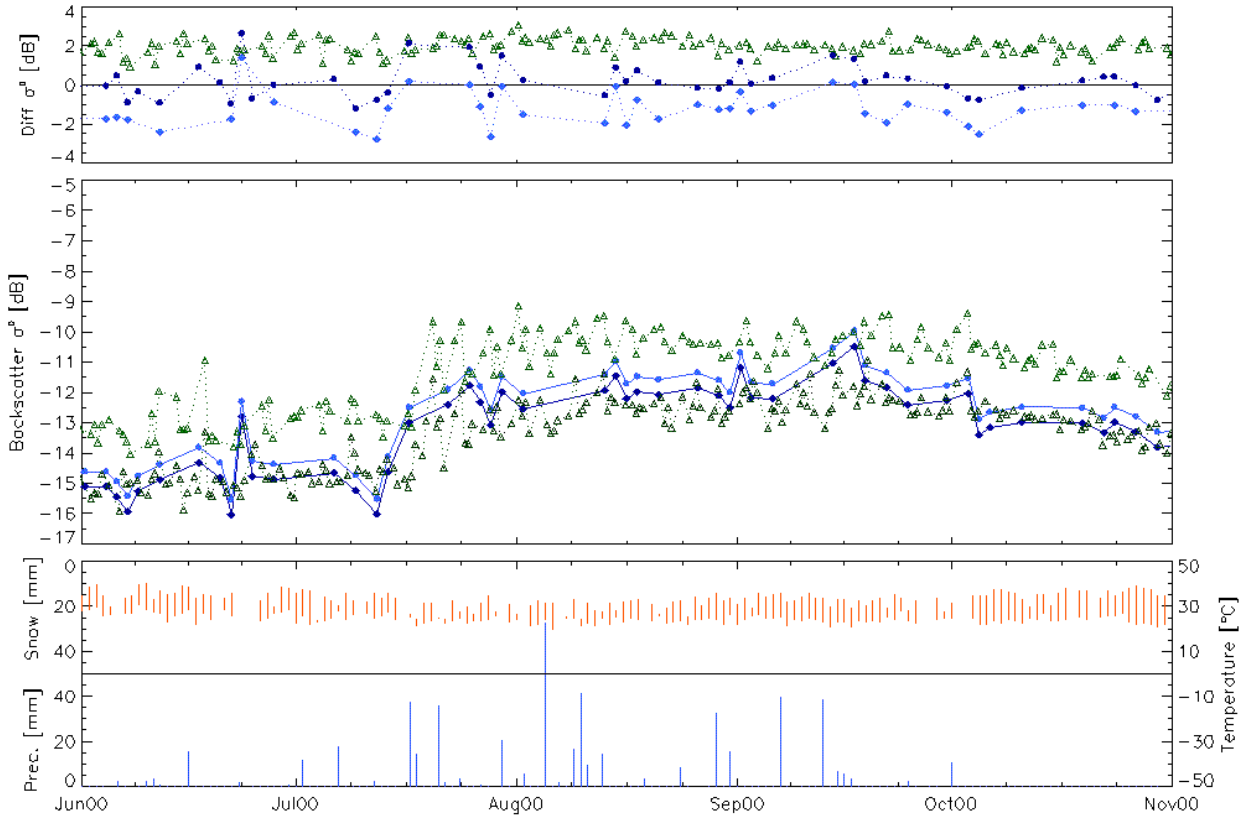

Fig.1. σ^0 and meteorological time series for San/Mali (4.1°W, 14.6°N). Bottom: synoptic meteorological data (minimum/maximum temperature and precipitation; Center: C-band $\sigma^0_{VV}(46)$ (blue dots) and $\sigma^0_{VV}(54)$ (dark blue diamonds), K_u-band $\sigma^0_{HH}(46)$ (green triangles) and $\sigma^0_{VV}(54)$ (dark green triangles); Top: difference C-band $\sigma^0_{VV}(46)$ and K_u-band $\sigma^0_{HH}(46)$ (blue dots), difference C-band $\sigma^0_{VV}(54)$ and K_u-band $\sigma^0_{VV}(54)$ (dark blue diamonds), K_u-band $\sigma^0_{HH}(46)$ and $\sigma^0_{VV}(54)$ (green triangles).

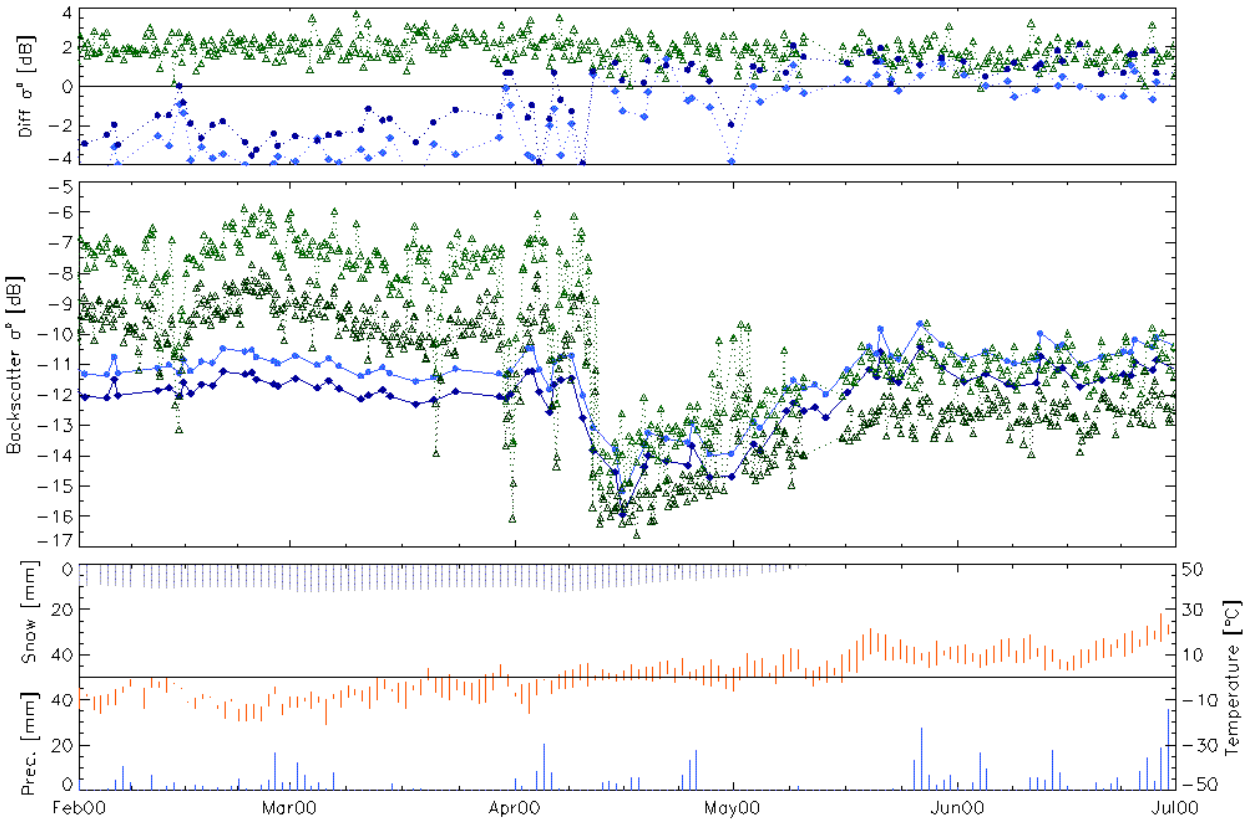

Fig. 2. Same as Fig. 1. but for Rovaniemi/Finland (25.8°E, 66.6°N).

The sharp decrease of backscatter in K_u-band when snow melts, indicates a smooth appearance of wet snow in the respective frequency. This effect is less pronounced for C-band, but still significant. After the onset of thawing C- and K_u-band backscatter decrease, followed by an increases until snow has totally disappeared. After that σ^0 remains stable during the remaining warm season. Contrary to the African Steppe, the difference between C- and K_u-band σ^0 is not so pronounced during the snow free period. C-band $\sigma^0_{VV}(46)$ and K_u-band $\sigma^0_{VV}(46)$ exhibit a similar backscatter intensity; C-band $\sigma^0_{VV}(54)$ and K_u-band $\sigma^0_{HH}(54)$ a constant offset of 1dB with higher C-band backscatter.

ACKNOWLEDGEMENT

This work has been supported through the Austrian Science Fund.

REFERENCE

[1] Tsai, W.-T., M. Spencer, C. Wu, C. Winn, K. Kellogg (2000) SeaWinds on QuikSCAT: sensor description and mission overview, *Proc. IGARSS' 2000,* Honolulu, Hawaii, 24-28 July 2000, pp.1021-1023.

[2] Walker, N.P (1997) Limitations on the possible resolution enhancement of ERS-1 scatterometer images, *IEEE Transactions on Geoscience and Remote Sensing*, Vol. 35, No. 1, pp. 196 –198

[3] Wagner W., J. Noll, M. Borgeaud, H. Rott (1999) Monitoring Soil Moisture over the Canadian Prairies with the ERS Scatterometer, *IEEE Trans. Geosci. Remote Sensing, Vol. 37, No. 1, pp. 206-216.*

[4] Mätzler, C. (1987) Applications of the Interaction of Microwaves with the Natural Snow cover, Remote Sensing Reviews, Vol. 2, pp. 259-387.